Available online at www.sciencedirect.com
SCIENCE DIRECT
Bioorganic & Medicinal Chemistry 14 (2006) 6608–6614
Bioorganic & Medicinal Chemistry

Membrane interaction of amphotericin B as single-length assembly examined by solid state NMR for uniformly ^{13}C-enriched agent

Shigeru Matsuoka,[a,b] Hiroki Ikeuchi,[a] Yuichi Umegawa,[a] Nobuaki Matsumori[a] and Michio Murata[a,*]

[a]*Department of Chemistry, Graduate School of Science, Osaka University, 1-16 Machikaneyama, Toyonaka, Osaka 560-0043, Japan*
[b]*CREST, Japan Science and Technology Corporation (JST), Osaka University, 1-16 Machikaneyama, Toyonaka, Osaka 560-0043, Japan*

Received 28 April 2006; revised 31 May 2006; accepted 1 June 2006
Available online 16 June 2006

Abstract—The membrane interaction of amphotericin B (AmB), one of the most important anti-fungal drugs, was investigated by solid state NMR measurements of uniformly ^{13}C-enriched AmB, which was prepared by the culture of the drug-producing microorganism in the presence of [u-$^{13}C_6$]glucose. All the ^{13}C NMR signals of AmB upon binding to DLPC membrane were successfully assigned on the basis of the ^{13}C–^{13}C correlation spectrum. ^{13}C–^{31}P RDX (Rotational-Echo Double Resonance for X-clusters) experiments clearly revealed the REDOR dephasing effects for carbon atoms residing in the both terminal parts, whereas no dephasing was observed for the middle parts including polyolefinic C20–C33 and hydroxyl-bearing C8/C9 parts. These observations suggest that AmB binds to DLPC membrane with a high affinity to the phospholipid and spans the membrane with a single molecular length.

1. Introduction

Amphotericin B (AmB, Fig. 1) has been clinically used for more than 40 years as one of the most efficacious antibiotics to treat fungal infections.[1,2] The therapeutic advantages of the drug are broad antimicrobial spectrum and characteristic action mechanism which hardly engender drug-resistant strains.[3] However, the clinical use of AmB is generally restricted to systemic infections owing to its serious side effects.[4,5] Recently, the importance of antifungal agents has been increasingly recognized because fungal infections are sometimes fatal for patients with the acquired immune deficiency syndrome (AIDS) and immune suppressions upon organ transplants.[6,7] AmB forms an ion-permeable channel across phospholipid membrane, which is thought to be responsible for the antibiotic activity.[8] The selective toxicity of AmB to fungus and other eukaryotic microbes is generally accounted for by an intermolecular recognition between AmB and membrane sterols;[9] in fungus membrane, ergosterol is a predominant sterol, while cholesterol is a major constituent of mammalian plasma membranes. It has been reported that the polar head moiety of AmB interacts with a hydroxyl group of sterol by hydrogen bonding, while the hydrophobic polyolefinic part comes close to the aliphatic rings of sterol.[10–14] The binding affinity of AmB to ergosterol is approximately one order of magnitude higher than that to cholesterol,[15] which is considered to be responsible for the selective toxicity of AmB against fungi. AmB is known to form an ion channel without sterols in phospholipid membrane.[16–27] Moreover, phospholipid composition is known to greatly influence the activity of AmB.[23–29] The interaction between AmB and phospholipids may, therefore, be as important as the AmB–sterol interaction for understanding the molecular-based mechanism of the drug.

We have recently reported that the membrane permeabilizing activity of AmB is greatly affected by the acyl chain length of saturated phosphatidylcholine (PC).[27] It is known that there are two types of ion channels formed by AmB, single-length and double-length assemblies, depending on the thickness of lipid bilayers as illustrated in Figure 2.[27,30,31] We have recently detected the inter-atomic interactions between the both terminal parts of AmB and the phosphate group of PC in

Keywords: Amphotericin B; Solid state NMR; REDOR; Phospholipid; Lipid bilayer.
* Corresponding author. Tel./fax: +81 66850 5774; e-mail: murata@ch.wani.osaka-u.ac.jp

0968-0896/$ - see front matter © 2006 Elsevier Ltd. All rights reserved.
doi:10.1016/j.bmc.2006.06.001

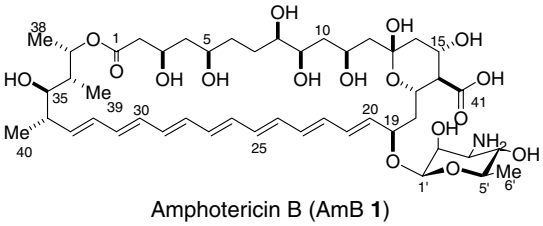

Figure 1. AmB and DLPC with carbon numbering.

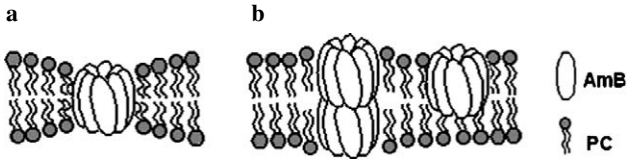

Figure 2. Schematic models for membrane interaction of AmB assembly with DLPC or DMPC (a) and DSPC (b) bilayer membranes.[32] The assembly of AmB is drawn as a barrel-stave model.[10]

dimyristoylphosphatidylcholine (DMPC) bilayers using solid state NMR techniques.[32] In that study, we carried out the ^{13}C–^{31}P rotational echo double resonance (REDOR)[34–36] experiments for a lipid dispersion of DMPC containing 39,40,41-$^{13}C_3$-labeled AmB.[32] These results provide the first spectroscopic evidence that AmB and DMPC form mainly the single-length type of a channel complex (Fig. 2).[32] We have also reported that the AmB–PC interaction is significantly affected by the acyl chain length of saturated PC;[27] the channel-forming activity of AmB is greatly enhanced by short-chained PCs (C_{10} and C_{12}) and markedly inhibited by long-chained PC (C_{18}). The ^{13}C–^{31}P REDOR experiments have further revealed that AmB fails to span across the thick bilayer of DSPC (C_{18}, distearoyl-PC)[32] (Fig. 2). We suppose that short-chained DLPC (C_{12}, dilauroyl-PC) should stabilize the molecular assembly better than DMPC, hence allowing us to selectively observe the AmB–PC interaction in a single-length assembly. In addition, proximity of carbon atoms to the phosphate of PC other than C39, C40, and C41 should more clearly reveal the membrane interaction of an AmB molecule. In the present study, we carried out solid state NMR experiments with a lipid dispersion of short-chained DLPC and uniformly enriched AmB (Fig. 1). We further report the applications of solid state NMR techniques to the complicated multiple spin system of uniformly ^{13}C-enriched AmB.

2. Materials and methods

2.1. Materials

1,2-Dilauroyl-*sn*-glycero-3-phosphocholine (DLPC) was purchased from Avanti Polar Lipid Inc. (Alabaster, AL). The surface-active agent, Aliquat 336® (Acros Organics), was purchased from Wako Pure Chemical Industries (Osaka, Japan). Uniformly ^{13}C-labeled D-glucose ([u-$^{13}C_6$]glucose, 98.8 atom%, Chlorella Industry Co.) was obtained from Shodex (Tokyo, Japan). All these chemicals were used without further purification.

2.2. Culture of *Streptomyces nodosus* and purification of AmB

The amphotericin B-producing strain *Streptomyces nodosus* obtained from American Type Culture Collection (ATCC 14899) was cultured to afford [u-^{13}C]AmB according to the procedure reported by McNamara et al.[33] with some important modifications. For the production culture, *S. nodosus* was grown on the 'FCA' [Fructose-Collofilm dextrin-Arkasoy (soy bean flower)] production medium containing fructose 20 g/L, dextrin 60 g/L, soy bean flower 30 g/L, and $CaCO_3$ 10 g/L (pH 7.0).[33] A 500-mL Erlenmyer flask containing the production medium (50 mL) was incubated at 26 °C with shaking at 200 rpm. [u-$^{13}C_6$]glucose (945 mg) was added to the medium nine times in aliquots of 105 mg in 200 μL sterile water over 68 h (24, 41, 45, 49, 65, 69, 73, 88, and 92 h). After incubation for 140 h, the broth was adjusted to pH 10.5 with 5 M NaOH (0.5/50 mL broth), and then 25 mL of ethyl acetate containing Aliquat 336 (7% w/v) was added. After stirring vigorously for 1 h (200 rpm), the broth was adjusted to pH 10.5 with 5 M NaOH. The organic phase separated by centrifugation (8000*g*, 10 min) was collected by decantation and placed at 4 °C for a week to precipitate AmB as yellow solids. The precipitate was collected by centrifugation, washed with acetone (3 mL), dry acetone (3 mL), and methanol (3 mL), followed by solvent evaporation under vacuum to give amorphous AmB.[33] For complete removal of Aliquat 336, AmB once dissolved in DMF (2 mL) containing acetic acid (25 mL, pH 4) was precipitated by addition of diethyl ether (10 mL).[32] Purified AmB was dried under vacuum to furnish an average of 38 mg of [u-^{13}C]AmB from 50 mL of the culture. The purity was checked by ^{13}C NMR (>95%). The average incorporation of ^{13}C was estimated to be 15% from the isotope pattern of ESI mass spectra.

2.3. Sample preparation for solid state NMR measurements

Lipid dispersions were prepared as described previously.[32] For preparation of AmB-bound membrane, 2.8 mg [u-^{13}C]AmB and 15 mg DLPC (1:8 in molar ratio) were dissolved in 2 mL $CHCl_3$/MeOH (2:1), and the solvent was removed under vacuum for 8 h. The membrane preparation was hydrated with 17.8 μL of 10 mM HEPES buffer (pH 7.0) under Ar then diluted

with 1 mL H_2O. After a few minute sonication, the lipid suspension was freeze-thawed and stirred vigorously to make multilamellar vesicles. The suspension was lyophilized, then rehydrated with D_2O (17.8 μL), which should be enough for formation of lamellar structures. The sample was packed into a ϕ 4-mm MAS rotor.

2.4. Solid state NMR measurements

All spectra were recorded at 75.315 MHz for ^{13}C (7.05 T) on a CMX300 (Varian/Chemagnetics, Palo-Alto, CA) spectrometer with the MAS frequency of 7000 ± 2 Hz. Rotor temperature was maintained at 30 ± 1°C by a temperature controller. The spectral width was 30 kHz. The B_1 fields of hard pulses for ^{1}H, ^{13}C, and ^{31}P nuclei were 96, 83, and 65 kHz, respectively. The contact time of CP was set to 2 ms. FIDs were acquired under the ^{1}H TTPM decoupling[37] with field strength of 96 kHz. The recycle delay was set to 5 s. The magnetization transfer by combined MLEV refocusing and C7 (CMR7) pulse sequence[38] was performed with 49 kHz of ^{13}C irradiation field under the 110 kHz of ^{1}H continuous wave decoupling for 571 μs (4 rotor cycles). The RDX spectrum was carried out by the pulse sequence reported by Mehta and Schaefer[39] and measured with the RAMP-CP.[40] The dephasing time was set to 35.4 ms (248 rotor cycles) in order to detect ^{13}C–^{31}P dipolar interactions within 0.8 nm[39] that were observed in the previous study.[32] The static ^{31}P NMR spectrum was recorded without MAS to confirm the phase status of DLPC in membrane preparations.

3. Results and discussions

3.1. Biosynthetic preparation of uniformly ^{13}C-enriched amphotericin B

In the previous study, we biosynthetically labeled carbon atoms at C39, C40, and C41 residing in the both ends of an AmB molecule by feeding *S. nodosus* with sodium [3-^{13}C]propionate.[32,33] This terminal-labeled AmB has proven useful for examining the interaction of AmB–PC in lipid bilayers.[32] In the present experiments, we attempted to selectively observe the single-length assembly of AmB (Fig. 2) using thinner membrane consisting of shorter-chained DLPC. For deducing the orientation of AmB in the membrane, we attempted to obtain carbon–phosphorus dipolar interactions as many as possible, particularly for the middle part of the molecule. To prepare multiple ^{13}C-labeled AmB, we attempted to enrich all the carbon atoms with ^{13}C isotope by feeding the producing organisms with uniformly ^{13}C-labeled glucose. The biosynthetic

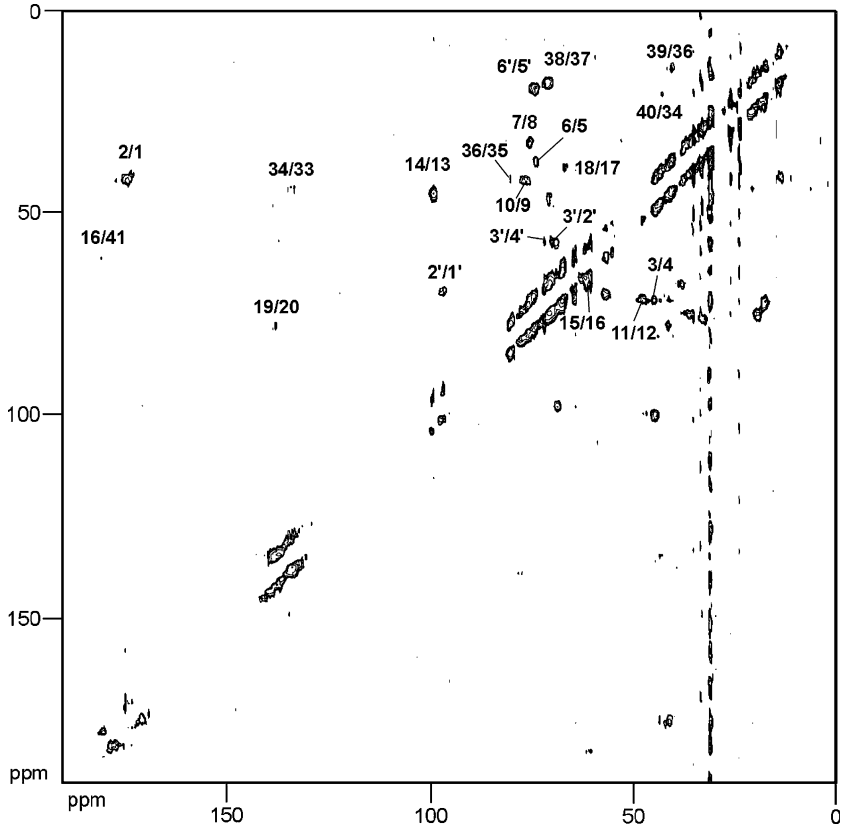

Figure 3. ^{13}C–^{13}C correlation spectrum. The DLPC membrane preparation contained the ^{13}C-enriched AmB at the AmB/DLPC molar ratio of 1:8 and 50 wt% 10 mM HEPES/D_2O buffer (pH 7.0). The spectra were obtained with the magic angle spinning at 7 kHz at 30 °C. The magnetization transfer by combined MLEV refocusing and C7 (CMR7) pulse sequence[38] was performed with 49 kHz of ^{13}C irradiation field under the 110 kHz of ^{1}H CW decoupling for 571 μs (4 rotor cycles). Assignments of cross peaks are provided in the spectrum with *m*/*n*; *m* corresponds to an F1 (vertical) signal, while *n* to F2 (horizontal).

preparation of the uniformly ^{13}C-enriched AmB ([u-^{13}C]AmB) was reported by McNamara et al.,[33] who used sodium [1,2-$^{13}C_2$]acetate as a feeding precursor. However, ^{13}C-abundance of their AmB was about 5%,[33] which should not be enough for our purpose. Since the other streptomyces products such as erythromycin A were reported to be more effectively labeled from [u-$^{13}C_6$]glucose,[38] we fed *S. nodosus* with the labeled glucose. The yield of [u-^{13}C]AmB was 38 mg from 50 mL of the 'FCA' production medium and the ^{13}C abundance was estimated at ca. 15% on the basis of the isotope pattern of the mass spectrum; the ESI mass spectrum of [u-^{13}C]AmB revealed that the weighted average of ^{13}C abundance for the broad distribution of isotope ion peaks was around *m*/*z* 953, which corresponded to $^{13}C_7{}^{12}C_{40}H_{73}O_{17}NNa$. Although AmB specimens with higher ^{13}C abundance, which gave rise to broader signals due to homo spin–spin coupling, were obtained by similar feeding experiments, the 15%-enriched lot was used in this experiment because higher resolution in a ^{13}C spectrum was essential for signal assignments in membrane.

3.2. ^{13}C NMR signal assignment by two-dimensional ^{13}C–^{13}C correlation spectra

We carried out solid state NMR experiments with a membrane preparation consisting of DLPC and [u-^{13}C]AmB (Fig. 1). Before ^{13}C signal assignments for AmB, we measured the magnitude of the chemical shift anisotropy of the static ^{31}P NMR signal of DLPC in membrane. The spectra revealed an axially symmetric pattern with the chemical shift anisotropy of 45 ppm and the line width at half-height of 1.5 kHz, which agreed well with the values of DMPC membrane in the liquid-crystalline (L_a) phase.[41] The signal pattern was virtually unchanged in the presence or absence of AmB. Besides, the line widths of ^{13}C signals in CP-MAS experiments ranged between 20 and 36 Hz, which matched those of DMPC in the L_a phase.[32] These results clearly demonstrate that the DLPC membrane containing 12.5 mol% of AmB is in the L_a phase. The ^{13}C NMR signals of [u-^{13}C]AmB were assigned on the basis of the two-dimensional version of a CMR7 pulse sequence[38] because CMR7 was one of the most efficient methods to build up magnetization transfers through homonuclear dipolar coupling at the MAS spinning rate of our experiments. Figure 3 shows the ^{13}C–^{13}C correlation spectrum of [u-^{13}C]AmB in the lipid dispersion of DLPC, where the ^{13}C signals of [u-^{13}C]AmB are completely separated on a two-dimensional plane. Some of ^{13}C–^{13}C pairs, however, gave rise to very weak or no cross-peaks. These C–C bonds correspond to the junctions among biosynthetic C_2 units such as acetate–acetate and acetate–propionate,[33] indicating that [u-$^{13}C_6$]glucose is converted to [1,2-$^{13}C_2$]acetate and [1,2,3-$^{13}C_3$]propionate before incorporated into AmB. Chemical shift data in a DMSO-d_6 solution[33] were partly utilized for the assignments of a few ^{13}C signals for which clear $^1J_{C,C}$ correlations could not be detected. The chemical shifts of all the carbon atoms of [u-^{13}C]AmB are shown in Table 1. Some ^{13}C signals were significantly shifted from those in a DMSO solution. In particular, the signals of hydroxy-bearing carbons C3, C5, and C11 were downfield-shifted over 2 ppm in the membrane; their δ_C values in DMSO have been reported to be 66.1, 69.7, and 67.7, respectively.[32] These shifts in δ_C values may be accounted for by the elimination of upfield-shifting effect by DMSO[43] and by formation of the intramolecular hydrogen-bonding, which is known to induce 1–2 ppm downfield shifts.[44] The unchanged chemical shifts of the rest of hydroxy-bearing carbon atoms may suggest that these hydroxyl groups including those in mycosamine are mostly hydrated. These notions may support the membrane-AmB interaction deduced from the RDX results (described later), in which the polyhydroxy C3–C11 part of AmB penetrates into membrane interior, while the polar head moiety and C35 hydroxyl group reside close to the membrane surfaces.

Table 1. Chemical shift* assignment of ^{13}C NMR for [u-^{13}C]AmB in DLPC (ppm)

Position	δ_c	Position	δ_c
1	171.0	19	75.6
2	39.5	20	136.7
3	69.1	21–32	130–140
4	43.5	33	134.3
5	72.3	34	41.7
6	34.9	35	79.0
7	31.0	36	39.2
8	74.2	37	69.9
9	75.0	38	15.7
10	39.9	39	11.9
11	69.7	40	19.0
12	46.0	41	178.5
13	97.5	1′	95.0
14	43.2	2′	67.9
15	65.5	3′	56.0
16	59.7	4′	68.7
17	65.9	5′	73.1
18	36.4	6′	17.9

The signal of AmB (C39) was taken as δ_c 11.9, which was a reported value for AmB in a DMSO-d_6 solution.[33]

3.3. [u-^{13}C]AmB–DLPC complex examined by ^{13}C–^{31}P REDOR for X clusters

Our strategy to investigate the interaction between AmB and DLPC was based on measurements of the ^{13}C–^{31}P intermolecular dipolar coupling between AmB and DLPC.[32] Conventional REDOR pulse sequences were not directly applicable to [u-^{13}C]AmB because of homonuclear coupling interactions arising from complicated ^{13}C spin networks in [u-^{13}C]AmB. In the original REDOR pulse sequence, the Hahn-echo is used for refocusing undesirable evolutions of observed nuclei during dephasing time before acquisition.[34,35] While chemical shifts and heteronuclear *J* coupling are refocused by Hahn-echo, homonuclear *J* coupling is not. The active coupling causes phase modulations in the REDOR spectra.[39] Schaefer's group and others have reported modified REDOR sequences that are applicable to homonuclear *J*-coupled spin systems.[32,42,45,46] Among those, REDOR for X clusters (RDX) was most suitable for our purpose because this experiment can refocus the homonuclear interactions of all signals without any effects of the heterogeneity in spin networks of observed

nuclei.[39] Since size of spin clusters is not known, quantitative evaluations of interatomic distances may be practically impossible in these experiments. However, it should be possible to compare the relative distances from phosphorus among dephased ^{13}C nuclei.

The RDX experiments were performed with ramped cross polarization[40] for ensuring constant initial ^{13}C magnetization during experimental time. In the spectrum shown in Figure 4, DLPC gives rise to narrow peaks, while [u-^{13}C]AmB shows broader resonances. Significant REDOR dephases were observed for some ^{13}C signals of the polar head group of DLPC (b–i, see Fig. 1 for the carbon labels). Based on the ^{13}C signal assignments (Table 1), the magnitude of the dephasing effect was compared among each part of AmB. The large dephasing was observed for the signals near the both terminal parts of an AmB molecule; in addition to the previously reported three carbons,[32] C39, C40, and C41, C1, C13, C35, C38, and C6′ revealed prominent dephases (Fig. 4). On the other hand, signals from the middle part of the molecule showed no evident dephasing; for example, the broad peaks of three oxygen-bearing carbon atoms C8, C9, and C19 gave rise to no prominent ΔS peaks, while small but significant dephasing effects were observed for C35 (and probably for C5′) as shown in the inset spectra of Figure 4. Moreover, the broad peak of 130–140 ppm corresponding to 14 double-bond carbon atoms also showed an only marginal dephase although a few of those in the edges of the heptane moiety should reside near the both ends of the AmB molecule (Fig. 4). These observations clearly demonstrate that the phosphate group of DLPC is located close to the both termini of AmB as is the case with DMPC membrane.[32] The magnitudes of dephasing for these eight signals are more than 10% (Table 2). It may be inappropriate to determine interatomic distances from the magnitudes of RDX dephasing (Table 2) because motional parameters and size of spin clusters of [u-^{13}C]AmB are not known.[47] However, we may be able to roughly estimate the distances by calculating the possible largest dipolar couplings between labeled carbon and phosphorus atoms. The normal REDOR attenuation for a ^{13}C–^{31}P pair separated by 0.82 nm is 51% after the dephasing time of 35.4 ms. The magnitude of REDOR dephasing of RDX is usually less than 50% of the normal REDOR dephasing during the initial rising period.[39] Since the dephasing magnitudes for C35, C39, C41, and C6′ are greater than 26%, the distance between each of these carbon and phosphorus should be smaller than 8.2 Å. This rough estimation implies that AmB spans DLPC membrane as depicted in Figure 2a. The lack of dephasing at the C8, C9, and most of heptane carbon atoms clearly indicates that the middle of the AmB molecule is embedded in membrane interior. Previously, we have reported that short-chained PCs

Table 2. Magnitude of ^{13}C–^{31}P REDOR dephasings, $\Delta S/S_0$ (%)

Position	$\Delta S/S_0$
1	15
13	32
35	32
38	21
39	26
40	18
41	30
6′	36

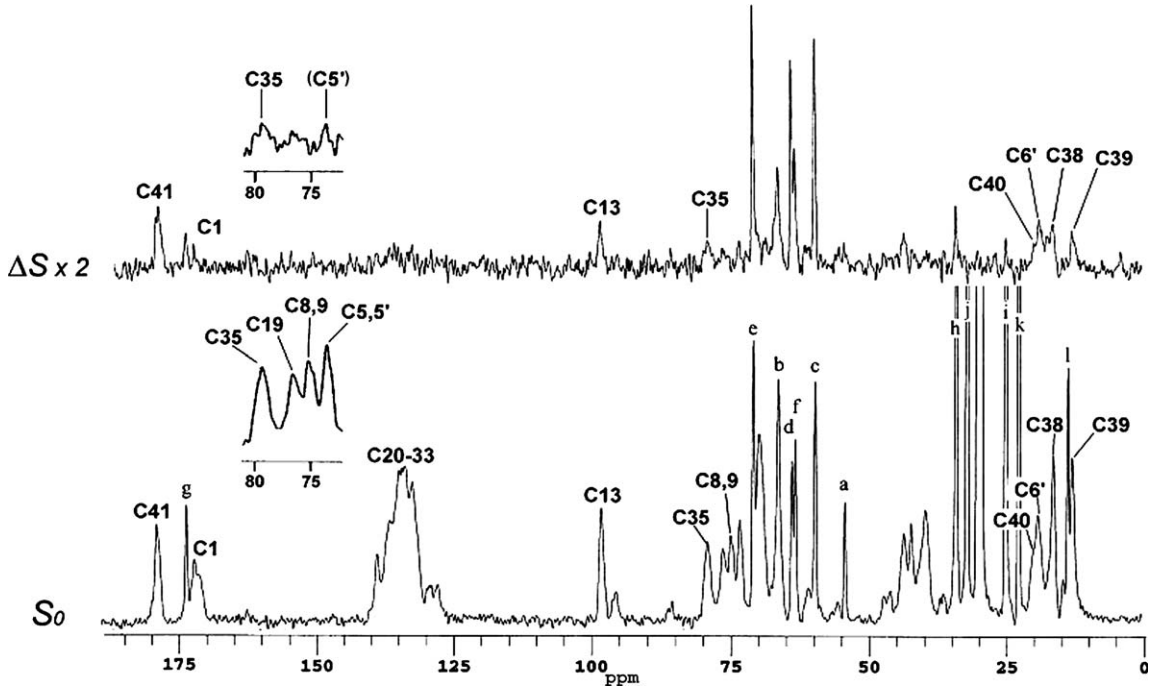

Figure 4. ^{13}C–^{31}P RDX spectrum of [u-^{13}C]AmB/DLPC. The same membrane preparation as that in Figure 3 was used. The spectra were obtained after 248 rotor cycles of ^{31}P dephasing (35.4 ms) with the magic angle spinning at 7 kHz at 30 °C. The number of the scans accumulated for the full echo spectrum, S_0, was 55,552. The top trace is the REDOR difference spectrum, ΔS. The insets show the expanded spectra for 72–82 ppm.

(C_{10} and C_{12}) promote membrane permeabilizing activity by AmB.[27] Based on the comparison of length of hydrophobic regions between AmB and PC bilayers, it is assumed that the ion-permeable channel formed by AmB has single molecular length and thinner hydrophobic regions of the short-chained DLPC facilitate AmB to span across the membrane with single molecular length.[27]

4. Conclusion

We examined the interaction between AmB and DLPC in membrane by solid state NMR using uniformly ^{13}C-enriched AmB. The chemical shifts of all carbon signals of membrane-bound AmB were successfully assigned on the basis of a ^{13}C–^{13}C correlation spectrum. With the signal assignments in hand, ^{13}C–^{31}P RDX experiments were carried out to confirm that AmB formed the single-length type of molecular assemblies in DLPC membrane. Although the precise structure of the ion channel remains unknown, the present study demonstrates that the solid sate NMR techniques in combination with uniformly ^{13}C-labeled molecules provide a useful method for investigating molecular complexes formed in lipid environments. Recently, we succeeded in improving the labeling percentage of [u-^{13}C]AmB up to 50%, and completing the chemical synthesis of ^{19}F-labeled AmB and sterols. Further investigations on the structure of molecular assembly formed by AmB and lipids are currently underway.

Acknowledgments

The present work was supported by Grants-in-Aid for Scientific Research (A) (No. 15201048), and for Scientific Research on Priority Area (A) (No. 16073211) from MEXT, Japan; by a grant from the CREST, Japan Science and Technology Corporation, and by the Yamada Science Foundation. We are grateful to Prof. Yuzuru Mikami, Research Center for Pathogenic Fungi and Microbial Toxicoses, Chiba University, for antifungal assays; to Prof. Tohru Oishi for discussion; and to Mutsuhiro Ohata and Satoru Ujihara for their help in cultures of microorganism.

References and notes

1. Gallis, H. A.; Drew, R. H.; Pickard, W. W. *Rev. Infect. Dis.* **1990**, *12*, 308–329.
2. Hann, I. M.; Prentice, H. G. *Int. J. Antimicrob. Agents* **2001**, *17*, 161–169.
3. Ellis, D. *J. Antimicrob. Chemother.* **2002**, *49*(Suppl. S1), 7–10.
4. Razzaque, M. S.; Hossain, M. A.; Ahsan, N.; Taguchi, T. *Nephron* **2001**, *89*, 251–254.
5. Deray, G. *J. Antimicrob. Chemother.* **2002**, *49*(Suppl. S1), 37–41.
6. Gupta, A. K.; Tomas, E. *Dermatol. Clin.* **2003**, *21*, 565–576.
7. Ablordeppey, S. Y.; Fan, P.; Ablordeppey, J. H.; Mardenborough, L. *Curr. Med. Chem.* **1999**, *6*, 1151–1195.
8. Bolard, J. *Biochim. Biophys. Acta* **1986**, *864*, 257–304.
9. Hartsel, S. C.; Bolard, J. *Trends Pharmacol. Sci.* **1996**, *17*, 445–449.
10. De Kruijff, B.; Demel, R. A. *Biochim. Biophys. Acta* **1974**, *339*, 57–70.
11. Andreoli, T. E. *Kidney Int.* **1973**, *4*, 337–345.
12. Herve, M.; Debouzy, J. C.; Borowski, E.; Cybulska, B.; Gary-Bobo, C. M. *Biochim. Biophys. Acta* **1989**, *980*, 261–272.
13. Baran, M.; Mazerski, J. *Biophys. Chem.* **2002**, *95*, 125–133.
14. (a) Matsumori, N.; Eiraku, N.; Matsuoka, S.; Oishi, T.; Murata, M.; Aoki, T.; Ide, T. *Chem. Biol.* **2004**, *11*, 673–679; (b) Matsumori, N.; Sawada, Y.; Murata, M. *J. Am. Chem. Soc.* **2005**, *127*, 10667–10675.
15. Readio, J. D.; Bittman, R. *Biochim. Biophys. Acta* **1982**, *685*, 219–224.
16. Milhaud, J.; Hartmann, M. A.; Bolard, J. *Biochimie* **1989**, *71*, 49–56.
17. Whyte, B. S.; Peterson, R. P.; Hartsel, S. C. *Biochem. Biophys. Res. Commun.* **1989**, *164*, 609–614.
18. Hartsel, S. C.; Benz, S. K.; Peterson, R. P.; Whyte, B. S. *Biochemistry* **1991**, *30*, 77–82.
19. Cohen, B. E. *Biochim. Biophys. Acta* **1992**, *1108*, 49–58.
20. Wolf, B. D.; Hartsel, S. C. *Biochim. Biophys. Acta* **1995**, *1238*, 156–162.
21. Cotero, B. V.; Rebolledo-Antunez, S.; Ortega-Blake, I. *Biochim. Biophys. Acta* **1998**, *1375*, 43–51.
22. Matsuoka, S.; Murata, M. . *Biochim. Biophys. Acta* **2002**, *1564*, 429–434.
23. HsuChen, C. C.; Feingold, D. S. *Biochem. Biophys. Res. Commun.* **1973**, *51*, 972–978.
24. Van Hoogevest, P.; De Kruijff, B. *Biochim. Biophys. Acta* **1978**, *511*, 397–407.
25. Cohen, B. E. *Int. J. Pharm.* **1998**, *162*, 95–106.
26. Ruckwardt, T.; Scott, A.; Scott, J.; Mikulecky, P.; Hartsel, S. C. *Biochim. Biophys. Acta* **1998**, *1372*, 283–288.
27. Matsuoka, S.; Murata, M. *Biochim. Biophys. Acta* **2003**, *1617*, 109–115.
28. Clejan, S.; Bittman, R. *J. Biol. Chem.* **1985**, *260*, 2884–2889.
29. Matsuoka, S.; Matsumori, N.; Murata, M. *Org. Biomol. Chem.* **2003**, *1*, 3882–3884.
30. Marty, A.; Finkelstein, A. *J. Gen. Physiol.* **1975**, *65*, 515–526.
31. Kleinberg, M. E.; Finkelstein, A. *J. Membr. Biol.* **1984**, *80*, 257–269.
32. Matsuoka, S.; Ikeuchi, H.; Matsumori, N.; Murata, M. *Biochemistry* **2005**, *44*, 704–710.
33. McNamara, C. M.; Box, S.; Crawforth, J. M.; Hickman, B. S.; Norwood, T. J.; Rawlings, B. J. *J. Chem. Soc., Perkin Trans. 1* **1998**, 83–87.
34. Gullion, T.; Schaefer, J. *J. Magn. Reson.* **1989**, *81*, 196–200.
35. Gullion, T.; Schaefer, J. *Adv. Magn. Reson.* **1989**, *13*, 57–83.
36. Hirsh, D. J.; Hammer, J.; Maloy, W. L.; Blazyk, J.; Schaefer, J. *Biochemistry* **1996**, *35*, 12733–12741.
37. Bennett, A. E.; Rienstra, C. M.; Auger, M.; Lakshmi, K. V.; Griffin, R. G. *J. Chem. Phys.* **1995**, *103*, 6951–6958.
38. Rienstra, C. M.; Hatcher, M. E.; Mueller, L. J.; Sun, B.; Fesik, S. W.; Griffin, R. G. *J. Am. Chem. Soc.* **1998**, *120*, 10602–10612.
39. Mehta, A. K.; Schaefer, J. *J. Magn. Reson.* **2003**, *163*, 188–191.
40. Metz, G.; Wu, X.; Smith, S. O. *J. Magn. Reson., Ser A* **1994**, *110*, 219–227.
41. Cullis, P. R.; De Kruyff, B.; Richards, R. E. *Biochim. Biophys. Acta* **1976**, *426*, 433–446.
42. Schaefer, J. *J. Magn. Reson.* **1999**, *137*, 272–275.

43. For example Kobayashi, Y.; Lee, J.; Tezuka, K.; Kishi, Y. *Org. Lett.* **1999**, *13*, 2177–2180.
44. (a) Jolibois, F.; Soubias, O.; Réat, V.; Milon, A. *Chem. Eur. J.* **2004**, *10*, 5996–6004; (b) Soubias, O.; Jolibois, F.; Réat, V.; Milon, A. *Chem. Eur. J.* **2004**, *10*, 6005–6014.
45. Jaroniec, C. P.; Tounge, B. A.; Rienstra, C. M.; Herzfeld, J.; Griffin, R. G. *J. Am. Chem. Soc.* **1999**, *121*, 10237–10238.
46. Jaroniec, C. P.; Tounge, B. A.; Herzfeld, J.; Griffin, R. G. *J. Am. Chem. Soc.* **2001**, *123*, 3507–3519.
47. Goetz, J. M.; Schaefer, J. *J. Magn. Reson.* **1997**, *127*, 147–154.